Magnetoelectric effect of three-phase core-shell-matrix particulate multiferroic composites

Hsin-Yi Kuo and Tzu-Sheng Wu

Citation: Journal of Applied Physics **111**, 054915 (2012); doi: 10.1063/1.3692385
View online: http://dx.doi.org/10.1063/1.3692385
View Table of Contents: http://scitation.aip.org/content/aip/journal/jap/111/5?ver=pdfcov
Published by the AIP Publishing

Magnetoelectric effect of three-phase core-shell-matrix particulate multiferroic composites

Hsin-Yi Kuo[a] and Tzu-Sheng Wu
Department of Civil Engineering, National Chiao Tung University, Hsinchu 300, Taiwan

(Received 25 September 2011; accepted 4 February 2012; published online 14 March 2012)

This paper studies the magnetoelectricity of a core-shell-matrix three-phase particulate composite made of piezoelectric (PE) and piezomagnetic (PM) phases. We propose a micromechanical model, the two-level recursive scheme in conjunction with Mori-Tanaka's method, to investigate the effective magnetoelectric coupling coefficients of the composite. We compare this micromechanical solution with those predicted by finite element analysis, which provides the benchmark results for a periodic array of inclusions. Both the magnitudes and trends between them are in good agreement. Based on this micromechanical approach, we show that, for the case of PE/PM/PM (core/shell/matrix) multiferroic composite, with a coating appropriate for the inhomogeneity, the effective magnetoelectric coupling can be enhanced many-fold as compared to the noncoated counterpart. Further, useful design principles are proposed for engineering magnetoelectric composites. © *2012 American Institute of Physics*. [http://dx.doi.org/10.1063/1.3692385]

I. INTRODUCTION

A variety of technological applications, including magnetic field sensors, magnetically controlled optoelectric devices, and magnetoelectric memories have motivated the study of magnetoelectric (ME) coupling in materials and composites.[1,2] The magnetoelectric coupling was predicted by Landau and Lifshitz[3] and observed by Astrov[4] and by Rado and Folen[5] over fifty years ago. However, the coupling is weak in single-phase materials, and this has motivated the study of composites of piezoelectric (PE) and piezomagnetic (PM) media. The idea is that the applied magnetic field causes a deformation of the piezomagnetic material, which in turn induces a deformation in the piezoelectric material, thereby inducing an electric field.

The performance of a piezoelectric/piezomagnetic composite depends on the micro-geometry of the phase, since one has to provide effective strain coupling and avoid electromagnetic shielding. This has motivated a number of micromechanical models to predict the effective moduli of multiferroic composites. For example, Nan[6] and Huang and Kuo[7] used the Green's function method to study a fibrous composite consisting of $BaTiO_3$ and $CoFe_2O_4$. For such transversely isotropic fibrous composites, Benveniste[8] derived exact connections among effective magnetoelectroelastic moduli based on a formalism of Milgrom and Shtrikman.[9] Particulate composites were investigated by Harshé *et al.*[10] using a cubic model. The classical Eshelby's approach and the mean-field Mori-Tanaka model have been generalized to multiferroic composites by Li and Dunn,[11,12] Huang,[13] Wu and Huang,[14] Huang and Zhou,[15] and Srinivas *et al.*[16] Nan *et al.*[2] provide an extensive review of the literature and the state of the art.

However, much of this work is for two-phase composites. Recently, some three-phase piezoelectric and piezomagnetic composites were made experimentally or theoretically to enhance the ME coupling.[17–26] Among the three-phase heterogeneous media, the coated inclusion composite is a special and interesting case. The coating, a thin layer of the third phase intervening between an inclusion and the matrix, may be due to mechanical imperfections or deliberated introduction. A relatively small volume fraction of interphase, however, may play a crucial role in determining the overall response of the composite. Available solutions of problems of this kind can be found in the papers by Kuo,[27] Kuo and Pan,[28] and Dinzart and Sabar.[29] Kuo[27] and Kuo and Pan[28] considered multiferroic composites with coated circular/elliptic fibers under anti-plane shear with in-plane electro-magnetic fields. They developed their solutions by extending the classical Rayleigh's formulation on periodic conductive composites. On the other hand, Dinzart and Sabar[29] used Green's functions techniques, interfacial operators, and Mori-Tanaka's model for solving the magneto-electro-elastic, inhomogeneous, coated inclusion problem.

In the work of Friebel *et al.*[30] they proposed two-level recursive scheme and two-step method together with Mori-Tanaka or double-inclusion mean-field models as the homogenization approaches to investigate the effective property of viscoelastic composites containing multiple phases of coated inclusions. This work concerns single fields. In this paper, we apply the two-level recursive scheme in conjunction with Mori-Tanaka method to multiple couple fields, specifically electrostatic, magnetostatic, and mechanical.

The plan of this article is organized as follows. We consider a composite medium made of piezoelectric and piezomagnetic phases arranged in a microstructure consisting of coated spheres in a matrix in Sec. II. We begin by considering the constitutive equations and field equations of this heterogeneous material in Sec. II A. In Sec. II B, a micromechanical model is proposed as the homogenization technique. For comparison, we consider periodic arrays by finite element analysis in Sec. III. The above methods are

[a]Author to whom correspondence should be addressed. Electronic mail: hykuo@mail.nctu.edu.tw.

illustrated in Sec. IV using composites of $BaTiO_3$, $CoFe_2O_4$, and Terfenol-D as the core, shell, and matrix phases, respectively. We first compare the predictions between the micromechanical approach and finite element analysis. Both magnitudes and trends are in good agreement. Following that, we improve the ME coupling effect by tuning the material parameters. We show that significant enhancement can be achieved with appropriate coating to the particles, and useful design principles are proposed to enhance the coupling effect.

II. MICROMECHANICAL MODEL

A. Basic equations

Consider a three-phase particulate composite made of piezoelectric and piezomagnetic materials. The composite is consisting of a continuous matrix phase, m, in which there are embedded inhomogeneities of a spherical core phase, c, and a shell phase, s, which represents a layer of coating that encapsulates each particle of the core phase (Fig. 1). The radii of the core and shell are a and b, respectively, and the ratio between them is defined as $\gamma \equiv a/b$. The general constitutive relations for the rth phase are given by[31]

$$\begin{aligned}\boldsymbol{\sigma}^{(r)} &= \mathbf{C}^{(r)}\boldsymbol{\varepsilon}^{(r)} - \mathbf{e}^{t(r)}\mathbf{E}^{(r)} - \mathbf{q}^{t(r)}\mathbf{H}^{(r)},\\ \mathbf{D}^{(r)} &= \mathbf{e}^{(r)}\boldsymbol{\varepsilon}^{(r)} + \boldsymbol{\kappa}^{(r)}\mathbf{E}^{(r)} + \boldsymbol{\lambda}^{t(r)}\mathbf{H}^{(r)},\\ \mathbf{B}^{(r)} &= \mathbf{q}^{(r)}\boldsymbol{\varepsilon}^{(r)} + \boldsymbol{\lambda}^{(r)}\mathbf{E}^{(r)} + \boldsymbol{\mu}^{(r)}\mathbf{H}^{(r)},\end{aligned} \tag{1}$$

where $\boldsymbol{\sigma}$, $\mathbf{D}$, and $\mathbf{B}$ are the stress, electric displacement, and magnetic flux, respectively; $\boldsymbol{\varepsilon}$, $\mathbf{E}$, and $\mathbf{H}$ are the strain, electric field, and magnetic field. $\mathbf{C}$, $\mathbf{e}$, and $\mathbf{q}$ denote the elastic stiffness, piezoelectric constant, and piezomagnetic moduli; $\boldsymbol{\kappa}$, $\boldsymbol{\mu}$, and $\boldsymbol{\lambda}$ denote the dielectric permittivity, magnetic permeability, and the magnetoelectric coefficient, respectively. The superscript t denotes the transpose of the matrix. When the standard matrix notation for tensors is adopted, we can rewrite the constitutive equations in a compact form as

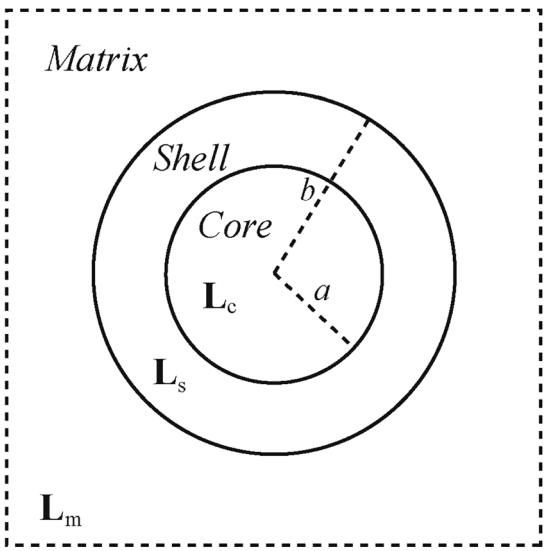

FIG. 1. The cross-section of a spherical, coated inclusion composite.

$$\boldsymbol{\Sigma} = \mathbf{L}\mathbf{Z}, \tag{2}$$

with

$$\boldsymbol{\Sigma} = \begin{bmatrix}\boldsymbol{\sigma}\\ \mathbf{D}\\ \mathbf{B}\end{bmatrix}, \mathbf{Z} = \begin{bmatrix}\boldsymbol{\varepsilon}\\ -\mathbf{E}\\ -\mathbf{H}\end{bmatrix}, \mathbf{L} = \begin{bmatrix}\mathbf{C} & \mathbf{e}^t & \mathbf{q}^t\\ \mathbf{e} & -\mathbf{k} & -\boldsymbol{\lambda}^t\\ \mathbf{q} & -\boldsymbol{\lambda} & -\boldsymbol{\mu}\end{bmatrix}. \tag{3}$$

The components of the strain ε, electric field $\mathbf{E}$, and magnetic field $\mathbf{H}$ are expressed in terms of the displacement $\mathbf{u}$, electric potential φ, and magnetic potential ψ by

$$\boldsymbol{\varepsilon} = \frac{1}{2}(\nabla\mathbf{u} + (\nabla\mathbf{u})^t), \quad \mathbf{E} = -\nabla\varphi, \quad \mathbf{H} = -\nabla\psi. \tag{4}$$

In the absence of body forces and electric and magnetic charges, the following equilibrium equations:

$$\nabla\cdot\boldsymbol{\sigma} = \mathbf{0}, \quad \nabla\cdot\mathbf{D} = \mathbf{0}, \quad \nabla\cdot\mathbf{B} = \mathbf{0} \tag{5}$$

must be satisfied. In addition to these differential equations, we have to use interface and boundary conditions. We assume that the interfaces are perfectly bonded, and therefore, the fields satisfy

$$[\![\boldsymbol{\sigma}\mathbf{n}]\!] = \mathbf{0}, [\![\mathbf{D}\cdot\mathbf{n}]\!] = 0, [\![\mathbf{B}\cdot\mathbf{n}]\!] = 0, [\![\mathbf{u}]\!] = \mathbf{0}, [\![\varphi]\!] = 0, [\![\psi]\!] = 0, \tag{6}$$

where $[\![\cdot]\!]$ denotes the jump in some quantity across the interface and $\mathbf{n}$ is the unit normal to the interface.

B. The effective moduli

In this study, we are interested in determining the macroscopic properties for a situation where we have a large number of inclusions. The effective properties of the composite are defined in terms of average fields,

$$\langle\boldsymbol{\Sigma}\rangle = \mathbf{L}^*\langle\mathbf{Z}\rangle, \tag{7}$$

where the angular brackets denote the average over the representative volume element (RVE; unit cell in the case of periodic composites),

$$\langle\boldsymbol{\Sigma}\rangle = \frac{1}{V}\int_V \boldsymbol{\Sigma}\mathbf{dx}, \langle\mathbf{Z}\rangle = \frac{1}{V}\int_V \mathbf{Z}\mathbf{dx},$$

and $\mathbf{L}^*$ denotes the effective magnetoelectroelastic parameters of the composite. Here, V is the volume of RVE. Note that, although in each component, the magnetoelectric coefficient is zero, i.e., $\boldsymbol{\lambda} = \mathbf{0}$, the coupling effect $\boldsymbol{\lambda}^*$ of the composite may be non-zero.

To estimate the effective moduli of multiferroic composites, we turn to a micromechanical model for this purpose. We first employ the two-level recursive scheme based on the idea that the matrix sees coated particles that are themselves composite. This procedure was first used to predict the behavior of viscoelastic composites containing multiple phases of coated inclusions.[30] As illustrated in Fig. 2, each coated particle is seen (deepest level) as a two-phase

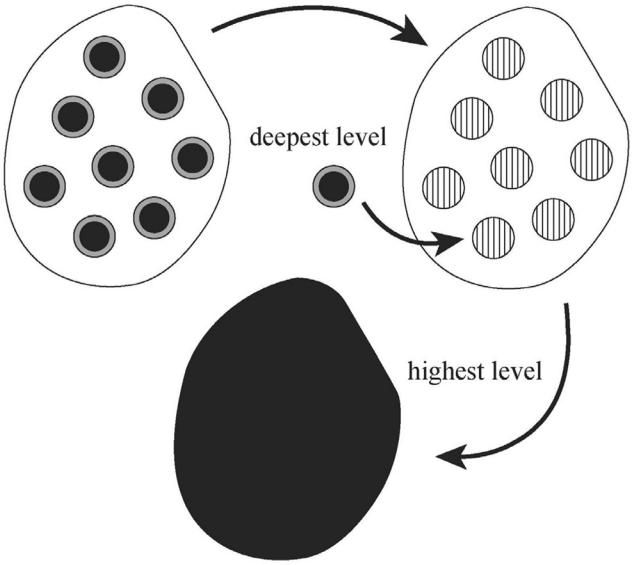

FIG. 2. The two-level recursive scheme. The coated particles are seen themselves as composites. Once homogenized (deepest level), they play the role of homogeneous inclusions for the matrix material (highest level) (Ref. 30).

composite, which, once homogenized, plays the role of a homogeneous inclusion for the matrix material (highest level).

Further, at each level, we resort to the Mori-Tanaka approach in predicting the effective moduli of the corresponding two-phase composites. The key assumption of the Mori-Tanaka model, which is essentially a mean-field method, is that the average field in the rth inclusion of the heterogeneous material is equivalent to the field in a single particle embedded in an infinite medium, with the unknown average field in the matrix applied at the boundary.[11,12] Using this model, at the deepest level, the coated inclusions are seen as a two-phase composite with effective moduli,

$$\mathbf{L}_{sc}^{*} = \mathbf{L}_s + \frac{f_c}{f_i}(\mathbf{L}_c - \mathbf{L}_s)\mathbf{A}_c^{MT}. \tag{8}$$

Here, f is the volume fraction, $\mathbf{A}^{MT}$ is the generalized strain concentration tensor, and the subscripts c, s, and i represent core, shell, and inclusion (core plus shell), respectively. The concentration tensor can be determined as

$$\mathbf{A}_c^{MT} = f_i \mathbf{A}_c^{dil}[f_s\mathbf{I} + f_c\mathbf{A}_c^{dil}]^{-1}, \tag{9}$$

with the dilute concentration tensor $\mathbf{A}_c^{dil}$ given by

$$\mathbf{A}_c^{dil} = [\mathbf{I} + \mathbf{S}_c\mathbf{L}_s^{-1}(\mathbf{L}_c - \mathbf{L}_s)]^{-1}, \tag{10}$$

where $\mathbf{I}$ is the identity matrix and $\mathbf{S}_c$ is the generalized Eshelby tensor for the core phase, which is a function of the magnetoelectroelastic moduli of the shell, and the shape and orientation of the core. For a fibrous or penny-shaped particle, the closed form expressions for this Eshelby tensor were derived by Li and Dunn.[11] For particles with spherical or more general shape, we turn to a numerical algorithm proposed by Li.[17]

At the highest level, the effective coated inclusions play the role of reinforcements and, similarly, we obtain the effective behavior

$$\mathbf{L}^{*} = \mathbf{L}_m + f_i(\mathbf{L}_{sc}^{*} - \mathbf{L}_m)\mathbf{A}_{sc}^{MT}, \tag{11}$$

where the subscript m denotes the matrix. Again, the concentration tensor can be determined as

$$\mathbf{A}_{sc}^{MT} = \mathbf{A}_{sc}^{dil}[f_m\mathbf{I} + f_i\mathbf{A}_{sc}^{dil}]^{-1}, \tag{12}$$

with the dilute concentration tensor

$$\mathbf{A}_{sc}^{dil} = [\mathbf{I} + \mathbf{S}_{sc}\mathbf{L}_m^{-1}(\mathbf{L}_{sc}^{*} - \mathbf{L}_m)]^{-1}. \tag{13}$$

Here, $\mathbf{S}_{sc}$ is the generalized Eshelby tensor for effective coated particles, which is a function of the moduli of the matrix and the shape and orientation of the coated inclusion (core plus shell).

III. FINITE ELEMENT ANALYSIS

In this section, we introduce finite element analysis, which is used for comparison with the above micromechanical approach. We first choose an appropriate representative volume element (RVE), a periodic unit cell which captures the major features of the underlying microstructure. There are fourteen lattice types to pack spheres a regular array in space.[32] Here, we concentrate on the cubic system, specifically, the face-centered cubic lattice.

Because of the periodicity in the composite structure, the displacement, $\mathbf{u}$, electric potential, φ, and magnetic potential, ψ, in any point of the unit cell can be expressed in terms of those at an equivalent point in another RVE, such that the following periodic boundary conditions should be satisfied:

$$\begin{aligned}
\Phi(d, x_2, x_3) &= \Phi(-d, x_2, x_3) + \langle \Phi_{,1} \rangle 2d, \\
\Phi(x_1, d, x_3) &= \Phi(x_1, -d, x_3) + \langle \Phi_{,2} \rangle 2d, \\
\Phi(x_1, x_2, d) &= \Phi(x_1, x_2, -d) + \langle \Phi_{,3} \rangle 2d.
\end{aligned} \tag{14}$$

Here, Φ can be the component of the displacement, $\mathbf{u}$, electric potential, φ, or the magnetic potential, ψ, and $2d$ is the side length of the unit cell. The comma in the subscript denotes the partial derivative.

To determine the effective properties of the above periodic multiferroic composite, the strain, $\boldsymbol{\varepsilon}$, electric field, $\mathbf{E}$, and magnetic field, $\mathbf{H}$, states are applied individually to the unit cell. The periodic boundary conditions have to be applied to the unit cell in such a way that, apart from one component of the strain, electric field, or magnetic field, $\langle \mathbf{Z} \rangle$, in (7), all other components are made equal to zero. For example, by applying a uniaxial strain state, say $\langle \varepsilon_{11} \rangle = 1$, and all of the other averaged terms to be zero, one can obtain the corresponding effective properties easily through (7).[20] We perform the finite element analysis using the software COMSOL Multiphysics.

IV. NUMERICAL RESULTS AND DISCUSSION

As a numerical example, we consider the case of a PE cores–coated PM shell in a PM matrix. We first choose $BaTiO_3$ (BTO) as the core phase, $CoFe_2O_4$ (CFO) as the

TABLE I. Material parameters of $BaTiO_3$,[12,33,34] $CoFe_2O_4$,[12] Terfenol-D,[35,36] and $LiNbO_3$.[33] (We assume the permeability of $LiNbO_3$ are the same as those of $BaTiO_3$.)

Property	$BaTiO_3$	$CoFe_2O_4$	Terfenol-D	$LiNbO_3$
C_{11}(GPa)	150.37	286	8.541	203
C_{12}(GPa)	65.63	173	0.654	52.9
C_{13}(GPa)	65.94	170.3	3.91	74.9
C_{33}(GPa)	145.52	269.5	28.3	243
C_{44}(GPa)	43.86	45.3	5.55	59.9
C_{66}(GPa)	43.37	56.5	18.52	74.9
C_{14}(GPa)	0	0	0	8.99
C_{56}(GPa)	0	0	0	8.985
$\kappa_{11}(nC^2/Nm^2)$	9.87	0.08	0.05	0.39
$\kappa_{33}(nC^2/Nm^2)$	11.08	0.093	0.05	0.26
$\mu_{11}(\mu Ns^2/C^2)$	5	590	8.644	5
$\mu_{33}(\mu Ns^2/C^2)$	10	157	2.268	10
$e_{15}(C/m^2)$	11.4	0	0	3.7
$e_{31}(C/m^2)$	−4.32	0	0	0.19
$e_{33}(C/m^2)$	17.36	0	0	1.31
$e_{16}(C/m^2)$	0	0	0	−2.534
$e_{21}(C/m^2)$	0	0	0	−2.538
q_{15}(N/Am)	0	550	155.56	0
q_{31}(N/Am)	0	580.3	−5.7471	0
q_{33}(N/Am)	0	699.7	270.1	0

shell phase, and Terfenol-D (TD) as the matrix phase and denote the composite as BTO/CFO/TD for simplicity. They are all transversely isotropic with 6 mm symmetry. The independent material constants are listed in Table I in Voigt notation.[12,33–36] Note that, in all materials, the magnetoelectric coefficients, $\boldsymbol{\lambda}$, are zero.

In our study, we are more interested in the effective magnetoelectric response. For the linear case of piezoelectric and piezomagnetic materials, the induced voltage is proportional to the applied magnetic field, and the constant of proportionality is the effective ME voltage coefficient. It combines the magnetoelectric and dielectric coefficients and is defined by $\alpha^*_{E,ij} = \lambda^*_{ij}/\kappa^*_{ij}$ (no summation). Specifically, we focus on the in-plane ME voltage coefficient $\alpha^*_{E,11}$ and the out-of-plane constant $\alpha^*_{E,33}$.

Figure 3 shows how the ME voltage coefficients depend on both the inclusion volume fraction, f_i, and the ratio of radii, γ, for the BTO/CFO/TD three-phase multiferroic composite. In the micromechanical approach, there is no upper limit on the volume fractions, since Mori-Tanaka's method is a mean-field theory. On the other hand, the finite element analysis is run for discrete volume fractions and stops around 0.74 when the inclusions touch. The overall magnitudes and trends agree well between the two approaches. The curves vary non-linearly with volume fraction, which initially increase with increasing volume fraction, then reach a maximum before dropping just as the coated inclusions close to fulfill the matrix. Further, the ME effect increases with increasing the ratio of radii, γ, for a fixed volume fraction before close to touching. For comparison, we also show the effective moduli of the composite made by the corresponding two-phase medium (BTO/TD). It shows that the ME voltage coefficient in the coated particulate composite can be indeed increased compared to its two-phase counterpart. In the former, the maximum coefficient $\alpha^*_{E,11}$ is −6.8 V/cmOe with $\gamma = 0.8$, and this is as much as *four* times higher than the value of −1.71 V/cmOe of the BTO/TD composite. For ME voltage coefficient $\alpha^*_{E,33}$, the maximum value of −5.5 V/cmOe is almost 1.7 times higher than −3.2 V/cmOe, which is the value of the corresponding two-phase composite.

Finally, Fig. 3 also compares the effective ME moduli with those predicted by the direct Mori-Tanaka method for the case $\gamma = 0.8$. The direct Mori-Tanaka method approximates the coated particle problem using a composite with distinct particles representing the core and shell phases. Following the standard derivation, one can show that

$$\mathbf{L}^* = \mathbf{L}_m + f_c(\mathbf{L}_c - \mathbf{L}_m)\mathbf{A}_1^{MT} + f_s(\mathbf{L}_s - \mathbf{L}_m)\mathbf{A}_2^{MT}, \qquad (15)$$

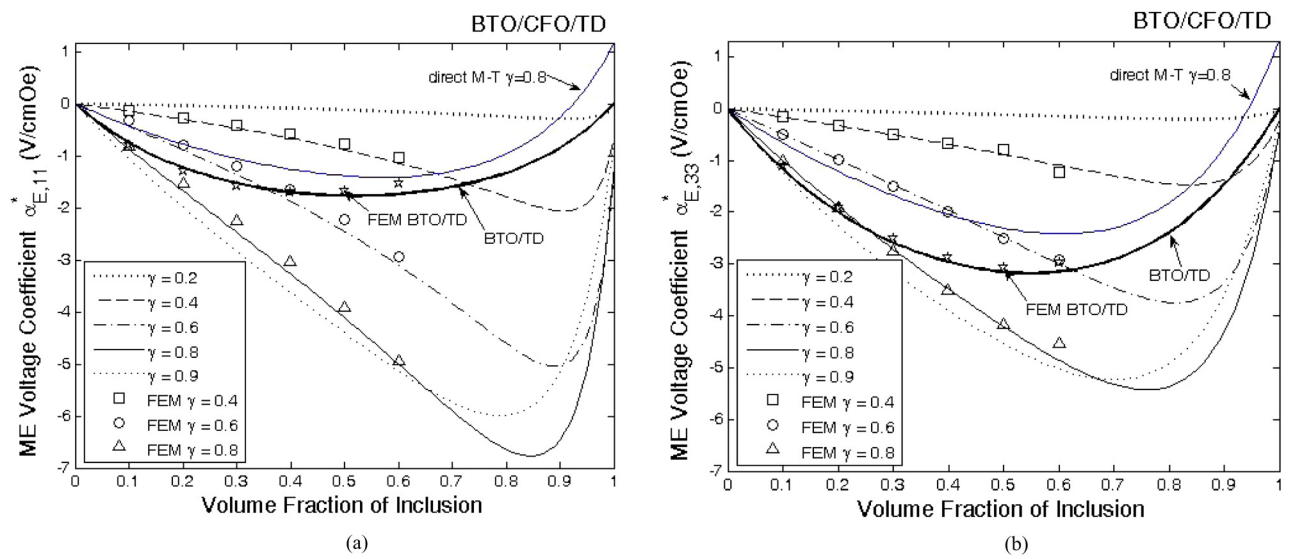

FIG. 3. (Color online) The predicted ME voltage coefficients vs the volume fraction of inclusion, f_i, and radius ratio, γ, of a BTO/CFO/TD (core/shell/matrix) three-phase composite: (a) ME voltage coefficient $\alpha^*_{E,11}$ and (b) ME voltage coefficient $\alpha^*_{E,33}$. In both (a) and (b), lines are based on the two-level recursive scheme with Mori-Tanaka's method, while discrete point symbols are based on the finite element analysis.

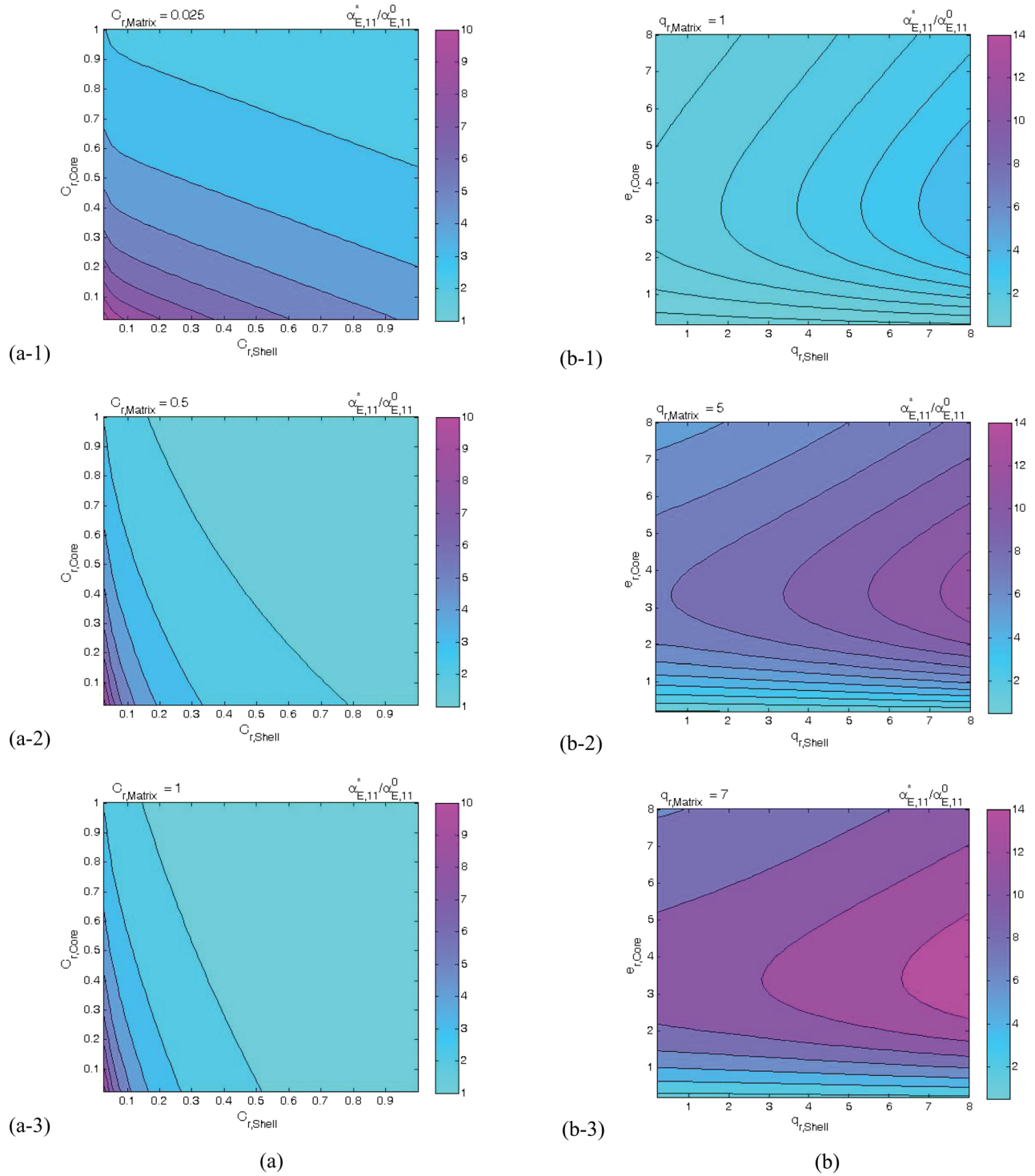

FIG. 4. (Color online) The predicted ME voltage coefficients vs different material parameters. The composite is made of piezoelectric core phase, piezomagnetic shell phase, and piezomagnetic matrix phase. The volume fraction of each phase is 1/3. The normalized ME voltage coefficient $\alpha^*_{E,11}/\alpha^0_{E,11}$ vs (a) normalized elastic constants $C_{r,Core}$, $C_{r,Shell}$, and $C_{r,Matrix}$; (b) normalized piezoelectric coefficient of PE core, $e_{r,Core}$, and piezomagnetic coefficients of PM shell, $q_{r,Shell}$, and matrix, $q_{r,Matrix}$; (c) normalized dielectric permittivities, $\kappa_{r,Core}$, $\kappa_{r,Shell}$, and $\kappa_{r,Matrix}$; and (d) normalized magnetic permeabilities, $\mu_{r,Core}$, $\mu_{r,Shell}$, and $\mu_{r,Matrix}$.

where

$$\mathbf{A}_j^{MT} = \mathbf{A}_j^{dil}(f_m\mathbf{I} + f_c\mathbf{A}_1^{dil} + f_s\mathbf{A}_2^{dil})^{-1}, \quad j = 1, 2,$$

and

$$\mathbf{A}_j^{dil} = [\mathbf{I} + \mathbf{S}_j\mathbf{L}_m^{-1}(\mathbf{L}_j - \mathbf{L}_m)]^{-1}.$$

Here, $\mathbf{S}_j$ again is the generalized Eshelby tensor, a function of the moduli of the matrix, and the shape and orientation of the core ($j = 1$) or shell ($j = 2$). It is observed that the prediction deviates largely from those determined by the finite element analysis. Therefore, the direct Mori-Tanaka method is not good in estimating the coupling constants, although calculations show that they evaluate elastic stiffness well.

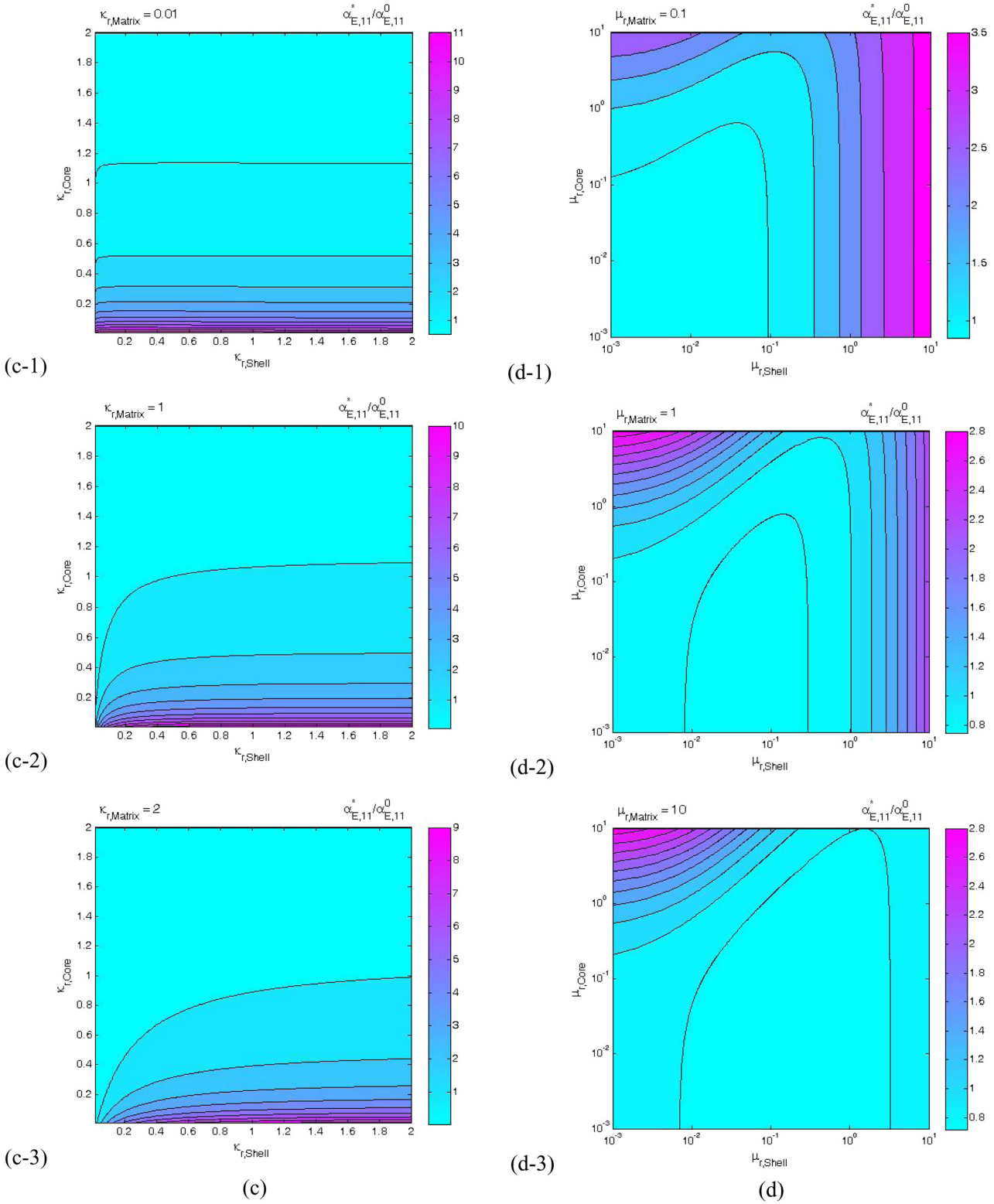

FIG. 4. *Continued.*

We now turn to study how the effective ME voltage coefficient depends on the elastic moduli, $\mathbf{C}_{PE}$ and $\mathbf{C}_{PM}$, dielectric permittivities, $\boldsymbol{\kappa}_{PE}$ and $\boldsymbol{\kappa}_{PM}$, and magnetic permeabilities, $\boldsymbol{\mu}_{PE}$ and $\boldsymbol{\mu}_{PM}$, of the PE and PM materials, piezoelectric coefficient, $\mathbf{e}_{PE}$, of the PE material, and piezomagnetic coefficient, $\mathbf{q}_{PM}$, of the PM material. For ease of comparison, we choose the material properties of BTO and CFO as the reference and define the normalized material properties of the PE and PM phases as

$$C_{r,Core}\mathbf{I} = \mathbf{C}_{PE}(\mathbf{C}_{BTO})^{-1}, C_{r,Shell}\mathbf{I} = \mathbf{C}_{PM}(\mathbf{C}_{CFO})^{-1},$$
$$C_{r,Matrix}\mathbf{I} = \mathbf{C}_{PM}(\mathbf{C}_{CFO})^{-1},$$

and, likewise, are $e_{r,Core}$, $q_{r,Shell}$, $q_{r,Matrix}$, $\kappa_{r,Core}$, $\kappa_{r,Shell}$, $\kappa_{r,Matrix}$, $\mu_{r,Core}$, $\mu_{r,Shell}$, and $\mu_{r,Matrix}$. Note that all the

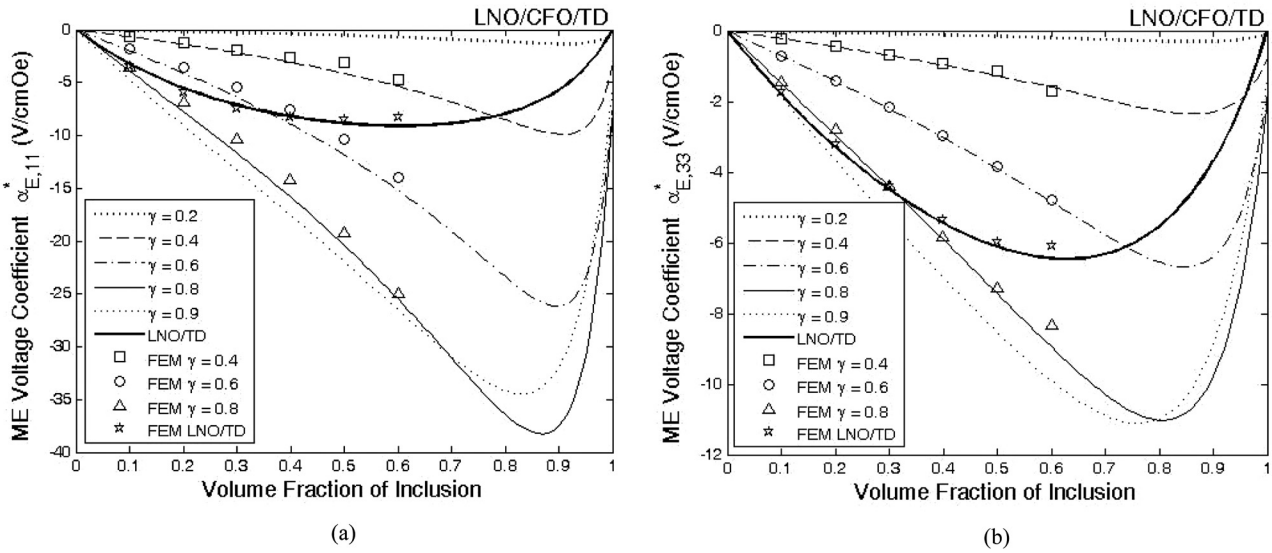

FIG. 5. The predicted ME voltage coefficients vs the volume fraction of inclusion, f_i, and radius ratio, γ, of a LNO/CFO/TD (core/shell/matrix) three-phase composite, (a) ME voltage coefficient $\alpha^*_{E,11}$, (b) ME voltage coefficient $\alpha^*_{E,33}$. In both (a) and (b), lines are based on the two-level recursive scheme with Mori-Tanaka's method, while discrete point symbols are based on the finite element analysis.

components of the material constant are magnified simultaneously for simplicity. Below, we numerically compute the ME voltage coefficient $\alpha^*_{E,11}$ and its dependence on the normalized material properties of core (PE), shell (PM), and matrix (PM) phases.

Figure 4 shows the contours of the relative effective ME voltage coefficient $\alpha^*_{E,11}/\alpha^0_{E,11}$ of a PE/PM/PM composite at the inclusion volume fraction, $f_i = 0.5$, and the ratio of the radii, $\gamma = 0.8$, where $\alpha^0_{E,11} = -1.3652$ V/cmOe, of BTO/CFO/CFO composite is chosen as the unit for the ME voltage coefficient, $\alpha^*_{E,11}$, for ease of comparison. In Fig. 4(a), the vertical and horizontal axes represent the normalized elastic constants of core and shell phases, while the variation of the matrix's elastic constant is shown by different subplots (a-1, a-2, and a-3). The other material constants are fixed, as those of BTO for PE phase or CFO for PM phase. It is observed that the ME voltage coefficient increases when any one of the core, shell, or matrix's elastic constant decreases. Therefore, softer PE and PM materials are preferred for improving the ME voltage coefficients of PE/PM/PM three-phase composites. Figure 4(b) shows the contours of the effective ME voltage coefficient versus the piezoelectric and piezomagnetic constants. For a fixed normalized piezoelectric coefficient, the ME voltage coefficient increases monotonically as either the shell or the matrix's piezomagnetic coefficient increases. However, for fixed normalized piezomagnetic coefficients of the shell and matrix phases, and as the piezoelectric coefficient increases, the coupling increases first and decreases after certain optimal $e_{r,Core} = 3.4$. Therefore, a larger piezomagnetic coefficient of either shell or matrix phase, but a nontrivial optimal piezoelectric constant are preferred for improving the ME effect of composites of three-phase multiferroic composites. Figure 4(c) shows the contours of the ME coupling versus the normalized electric permittivities of PE and PM phases. We observe that the smaller the PE core's permittivity, the larger the ME voltage coefficient. However, the PM permittivities, $\kappa_{r,Shell}$ and $\kappa_{r,Matrix}$, do not influence the ME effect much. Figure 4(d) shows the contours of the coupling constant versus the normalized magnetic permeabilities in logarithmic scale. We observe that increasing the PE core's and PM shell's magnetic permeabilities enhances the ME voltage coefficient, and on the contrary, increasing the PM matrix's magnetic permeability, $\mu_{r,Matrix}$, lowers the ME voltage coefficient. However, for the piezoelectric phase, which is not magnetically ordered, the smaller permeability does not influence the ME coupling much. For example, as $\mu_{r,Core} = 10^{-6}$, $\mu_{r,Shell} = \mu_{r,Matrix} = 1$, we have $\alpha^*_{E,11}/\alpha^0_{E,11} = 0.98878$.

Motivated by the above study, we do a similar calculation for $LiNbO_3$ (LNO), $CoFe_2O_4$, and Terfenol-D as the core, shell, and matrix phases, since LNO has lower dielectric permittivity and the matrix TD has lower elastic stiffness and magnetic permeability. The material constants of LNO are listed in Table I. Figure 5 shows the ME voltage coefficients, volume fraction, and ratio of radii dependence of LNO/CFO/TD. Significantly, the maximum values are enhanced to -38 V/cmOe and -11V/cmOe for $\alpha^*_{E,11}$ and $\alpha^*_{E,33}$, respectively.

V. CONCLUSIONS

In this work, we have proposed a micromechanical approach, the two-level recursive scheme in conjunction with the Mori-Tanaka method, to compute the effective magnetoelectric response of a core-shell-matrix, three-phase, multiferroic particulate composite. The results are compared with finite element analysis, and the magnitudes and trends between them are in good agreement. We have used it to show that, for the three-phase ME composite, as in the core-shell-matrix setting, the magnetoelectric response can be enhanced by more than an order of magnitude, as compared to the corresponding two-phase counterpart. In addition, for a PE/PM/PM three-phase multiferroic composite with fixed volume fraction and radius ratio, we show that softer materials are desirable for improving the ME voltage coefficient. It

is desirable to have larger piezomagnetic coefficient and magnetic permeability in the PM shell, larger piezomagnetic coefficient, but smaller magnetic permeability in the PM matrix, and smaller dielectric permittivity, but larger magnetic permeability in the PE core. Further, there exists an optimal value of the piezoelectric coefficient of the PE cores for maximum ME coupling.

In our model, we neglect the low resistance of the magnetic phase compared to the piezoelectric one. The eddy current loss for the magnetic phase can be high, and this may also result in an inefficient magnetoelectric energy conversion, especially in the high-frequency system.[26,37,38] However, the loss plays a less significant role in the static case, as we considered here. Further, for the magnetic phase made of a variety of ferrites, which are ferrimagnetic oxides and therefore are electrically insulating,[39] our model can reasonably estimate the overall behavior. At the same time, since the response is frequency-dependent, the analysis becomes significantly more involved. This remains an issue for future work.

ACKNOWLEDGMENTS

We are grateful to acknowledge the support under Grant Number NSC 100-2628-E-009-022-MY2.

[1]W. Eerenstein, N. D. Mathur, and J. F. Scott, Nature **442**, 759 (2006).
[2]C.-W. Nan, M. I. Bichurin, S. Dong, D. Viehland, and G. Srinivasan, J. Appl. Phys. **103**, 031101 (2008).
[3]L. D. Landau and E. M. Lifshitz, *Electrodynamics of Continuous Media* (Pergamon, New York, 1984), p. 119.
[4]D. N. Astrov, Sov. Phys. JETP **11**, 708 (1960).
[5]G. T. Rado and V. J. Folen, Phys. Rev. Lett. **7**, 310 (1961).
[6]C.-W. Nan, Phys. Rev. B **50**, 6082 (1994).
[7]J. H. Huang and W.-S. Kuo, J. Appl. Phys. **81**, 1378 (1997).
[8]Y. Benveniste, Phys. Rev. B **51**, 16424 (1995).
[9]M. Milgrom and S. Shtrikman, Phys. Rev. A **40**, 1568 (1989).
[10]G. Harshé, J. P. Dougherty, and R. E. Newnham, Int. J. Appl. Electromagn. Mater. **4**, 145 (1993).
[11]J. Y. Li and M. L. Dunn, Philos. Mag. A **77**, 1341 (1998).
[12]J. Y. Li and M. L. Dunn, J. Intell. Mater. Syst. Struct. **9**, 404 (1998).
[13]J. H. Huang, Phys. Rev. B **58**, 12 (1998).
[14]T.-L. Wu and J.-H. Huang, Int. J. Solids Struct. **37**, 2981 (2000).
[15]H. Huang and L. M. Zhou, J. Phys. D: Appl. Phys. **37**, 3361 (2004).
[16]S. Srinivas, J. Y. Li, Y. C. Zhou, and A. K. Soh, J. Appl. Phys. **99**, 043905 (2006).
[17]J. Y. Li, Int. J. Eng. Sci. **38**, 1993 (2000).
[18]J. Aboudi, Smart Mater. Struct. **10**, 867 (2001).
[19]C.-W. Nan, L. Liu, N. Cai, J. Zhai, Y. Ye, Y. H. Lin, L. J. Dong, and C. X. Xiong, Appl. Phys. Lett. **81**, 3831 (2002).
[20]J. Lee, J. G. Boyd IV, and D. C. Lagoudas, Int. J. Eng. Sci. **43**, 790 (2005).
[21]X. Wang and E. Pan, Phys. Rev. B **76**, 214107 (2007).
[22]A. Gupta and R. Chatterjee, J. Appl. Phys. **106**, 024110 (2009).
[23]K. H. Chau, Y. W. Wong, and F. G. Shin, Appl. Phys. Lett. **94**, 202902 (2009).
[24]P. A. Jadhava, M. B. Shelara, and B. K. Chougule, J. Alloys Compd. **479**, 385 (2009).
[25]E. Pan, X. Wang, and R. Wang, Appl. Phys. Lett. **95**, 181904 (2009).
[26]H. M. Wang, E. Pan, and W. Q. Chen, J. Appl. Phys. **107**, 093514 (2010).
[27]K.-Y. Kuo, Int. J. Eng. Sci. **49**, 561 (2011).
[28]H.-Y. Kuo and E. Pan, J. Appl. Phys. **109**, 104901 (2011).
[29]F. Dinzart and H. Sabar, Int. J. Solids Struct. **48**, 2393 (2011).
[30]C. Friebel, I. Doghri, and V. Legat, Int. J. Solids Struct. **43**, 2513 (2006).
[31]V. I. Alshits, A. N. Darinskii, and L. Lothe, Wave Motion **16**, 265 (1992).
[32]C. Kittel, *Introduction of Solid State Physics* (Wiley, New Jersey, 2005), p. 9.
[33]See http://www.efunda.com/home.cfm for information about $BaTiO_3$ and $LiNbO_3$.
[34]E. Pan, J. Appl. Mech. **68**, 608 (2001).
[35]D. Engdahl, *Handbook of Giant Magnetostrictive Materials* (Academic, San Diego, 2000), p. 175.
[36]C.-W. Nan, M. Li, and J. H. Huang, Phys. Rev. B **63**, 144415 (2001).
[37]M. I. Bichurin, D. A. Filippov, V. M. Petrov, V. M. Laletsin, N. Paddubnaya, and G. Srinivasan, Phys. Rev. B **68**, 132408 (2003).
[38]M. I. Bichurin, V. M. Petrov, S. V. Averkin, and E. Liverts, J. Appl. Phys. **107**, 053904 (2010).
[39]N. Spaldin, *Magnetic Materials: Fundamentals and Device Applications* (Cambridge University Press, Cambridge, 2003), p. 113.